ChemComm

CrossMark
← click for updates

Symmetry breaking above room temperature in an Fe(II) spin crossover complex with an N₄O₂ donor set†

Wasinee Phonsri,[a] Casey G. Davies,[b] Guy N. L. Jameson,[b] Boujemaa Moubaraki,[a] Jas S. Ward,[c] Paul E. Kruger,[c] Guillaume Chastanet[d] and Keith S. Murray*[a]

[Fe(qsal-Cl)₂] is one of the few known Fe(II) spin crossover compounds with an N₄O₂ donor atom environment. It shows an abrupt two-step spin transition at 308 and 316 K and importantly, symmetry breaking at the highest temperature reported, to date, in spin crossover compounds.

The study of spin crossover (SCO) materials continues to generate a great deal of interest from both fundamental and applied perspectives.[1–6] Fe(II) d⁶ and Fe(III) d⁵ compounds remain the metal systems of choice in these studies. Within these systems, mixed N/O-ligand donor sets are well known for Fe(III) but rare for Fe(II) SCO complexes.[7–16] Specifically, the qsal ligands are known to produce SCO with Fe(III).[12,17–20] However, only one qsal derivative of Fe(II), [Fe^II(qsal-NO₂)₂] (qsal-NO₂ = 5-nitro-N-(8-quinolyl)-salicylaldimine), has been reported to show SCO (incomplete) up to 400 K.[21] Generally, the space group symmetry of SCO compounds is unchanged following transition between different spin states. There are a limited number of compounds for which symmetry breaking takes place and accompanies complete SCO.[22–25] Notably, there are only two compounds that have shown symmetry breaking in an [Fe^IIN₄O₂] system *i.e.* Fe(II) with a hexadentate N₄O₂ ligand, [Fe(5-NO₂-sal-N(1,4,7,10))].[26] This compound shows two-step SCO with $T_{1/2}$ (heating) = 136 and 171 K, and three different space groups at 103, 153 and 292 K. Another example is a 1D chain of [FeL1(azpy)] where L1 is

the tetradentate N₂O₂ ligand (L1 = diethyl(*E*,*E*)-2,2′-[1,2-phenyl-bis(iminomethylidyne)]bis[3-oxobutanoate]-(2-)-*N*,*N*′,O³,O³′).[27] Herein, we report the first example of symmetry breaking with re-entrant behaviour in a complex containing a tridentate N₂O ligand, *viz.* [Fe(qsal-Cl)₂] **1**. Interestingly, **1** shows complete, abrupt two-step SCO above room temperature, the highest temperature yet reported so far for a mononuclear SCO compound.

Complex **1** was synthesized by a multi-layering method: a dichloromethane solution of Hqsal-Cl and Et₃N formed the bottom layer; neat MeOH formed the middle 'buffering' layer; whilst FeCl₂·4H₂O in MeOH formed the top layer. Black crystals formed in good yield within one week. Variable-temperature single crystal X-ray diffraction experiments on **1** were obtained at six temperatures, *viz.* 100, 298, 308, 312, 318 and 330 K that encompass all the different spin states observed (*vide infra*), Fig. 1.‡ Intriguingly, crystals of **1** show symmetry breaking. At 100 and 298 K, **1** exists in the monoclinic space group $P2_1/n$ and a single molecule of **1** is observed in the asymmetric unit. Between 308 and 312 K, the cell parameters α and γ deviate

[a] *School of Chemistry, Monash University, Clayton, Victoria, 3800, Australia. E-mail: keith.murray@monash.edu*

[b] *Department of Chemistry & MacDiarmid Institute for Advanced Materials and Nanotechnology, University of Otago, PO Box 56, Dunedin, 9054, New Zealand*

[c] *Department of Chemistry & MacDiarmid Institute for Advanced Materials and Nanotechnology, University of Canterbury, Private Bag 4800, Christchurch 8041, New Zealand*

[d] *CNRS, Université de Bordeaux, ICMCB, 87 avenue du Dr A. Schweitzer, Pessac 33608, France*

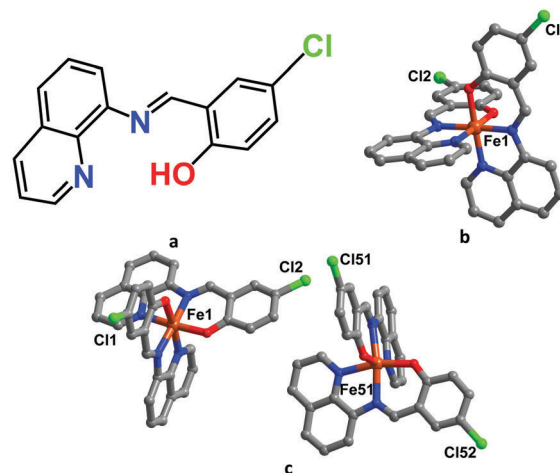**Fig. 1** Molecular structures of (a) Hqsal-Cl ligand and the asymmetric unit of **1** at (b) LS and HS state (c) intermediate states.

significantly from 90° and the symmetry changes to triclinic, $P\bar{1}$. At this intermediate stage (IP), there are two molecules of **1** in the asymmetric unit (labelled Fe1 and Fe51) with different spin states (1LS–1HS), Fig. 1c. At temperatures above 318 K, the crystal system reverts to $P2_1/n$, thus showing re-entrant behaviour.

The Fe(II) centres coordinate to N_4O_2 donors from two tridentate anionic qsal-Cl ligands chelating in meridional fashion to yield neutral **1**. Fe–L bond lengths for the compound are shown in Table S2 (ESI†). At 100 and 298 K, Fe–L distances (Fe–O $\approx$ 1.96 and Fe–N $\approx$ 1.94–1.99 Å) and the octahedral distortion parameters[28,29] ($\Sigma \approx 33°$ and $\Theta = 65$–74°) indicate that the Fe(II) centre is in the LS state.[30,31] Upon warming the crystal of **1** to between 308 and 312 K, there are two molecules in the asymmetric unit. The Fe–L bond lengths and octahedral distortion parameters suggest an intermediate state consisting of 1LS and 1HS Fe(II) centre in the asymmetric unit. At temperatures above 318 K only one molecule of **1** is again observed in the asymmetric unit, suggesting the fully HS structure exists at 330 K (Fe–O $\approx$ 2.01 and Fe–N $\approx$ 2.16 Å).

Although symmetry breaking is observed in **1**, the packing of the Fe(II) moieties within the crystal remains unchanged, Fig. 2. The supramolecular arrangements that remain similar during the symmetry breaking have also been reported in previous systems.[32–34] The deficiency of diffuse scattering and the extra Bragg reflections in the IP of compound **1** suggest that the spin transition relates to the long-range order characteristic of the IP.[24]

The packing in **1** is reminiscent of those seen in Fe(III)-qsal systems (albeit without the presence of an anion).[12,35–38] Thus, a chain of Fe(II) moieties interact through two sets of π–π interactions *via* sal···quin rings of the qsal-Cl ligands and C–H···O interactions along the *b* axis (Fig S1, ESI†). Moreover, along the *a* axis, C–H···Cl interactions and two sets of parallel fourfold aryl embraces (P4AE)[39] are observed to link the Fe moieties into higher dimension. P4AE is believed to be the reason for the observation of complete abrupt spin crossover in **1**[12,40] (see Magnetic section). Furthermore, in the *ac* plane, there are two extra sets of π–π interactions holding the Fe

Fig. 2 Simplification of symmetry breaking showing the molecules in the asymmetric unit as well as the packing of **1**, deep blue molecules in the unit cell packing represent fully LS state, orange and light blue molecules are in mostly HS and LS state, respectively and red is fully HS state of Fe(II).
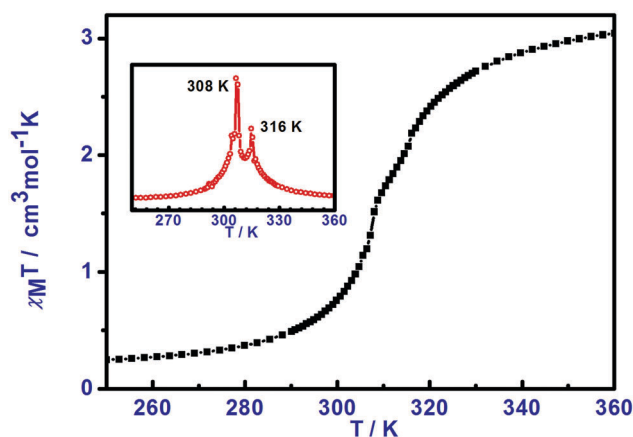

Fig. 3 Variable-temperature magnetic susceptibility ($\chi_M T$) measurements for compound **1**, an inset shows the first order differentiation of the magnetic plot.

molecules in the plane. It is important to note that two types of P4AE interactions and the extra two sets of π–π interactions described here are not seen in Fe(III)-(qsal-X) complexes. That is because anions and/or solvents occupy spaces between the [Fe(III)(qsal-Cl)$_2$] molecules and prevent those interactions taking place in those complexes. Such interactions are believed to be responsible for the greater cooperativity as they enhance the surface contacts between Fe(II) moieties.[41] Therefore, they result in the exceptionally high spin transition temperatures observed in **1** (*vide infra*).

The variable-temperature magnetic susceptibility data for **1** were obtained between 100–360 K using various scan rates *i.e.* 2, 5 and 10 K min^{-1}. The magnetic results for the compound are independent of the scan rate and are illustrated in Fig. 3. Upon closer inspection, together with differential scanning calorimetry results, two steps have been detected in **1** with a *pseudo*-plateau of width of about 8 K. Upon heating from 100 up to 250 K, the $\chi_M T$ values of **1** is invariant with temperature, with $\chi_M T$ values of about 0.3 cm^3 K mol^{-1}, indicative of the LS Fe(II) forms. Upon further warming, spin crossover takes place and **1** shows a two-step transition with $T_{1/2}$ = 308 and 316 K for the 1st and 2nd steps, respectively, before reaching the fully HS form at high temperatures. There is a small thermal hysteresis of about 1–2 K width present in this compound. The magnetic profiles are reproducible in subsequent cycles.

Variable temperature single crystal X-ray diffraction indicates concerted SCO and symmetry breaking in **1** *via* LS($P2_1/n$) $\leftrightarrow$ 1LS–1HS($P\bar{1}$) $\leftrightarrow$ HS($P2_1/n$) steps. This also agrees with the discontinuous changes of the unit cell parameters around 300 K (Fig S2, ESI†). Thus, there is a strong correlation between SCO and structural changes in this compound.

According to the reviewed information in Table S4 (ESI†), there is only a small number of examples of symmetry breaking with complete, two steps SCO that have been characterized. To the best of our knowledge, [Fe(qsal-Cl)$_2$] is the first Fe(II) complex with a N_2O ligand donor set that exhibits symmetry breaking involving a two-step SCO, above RT, the highest temperatures reported for symmetry breaking in mononuclear
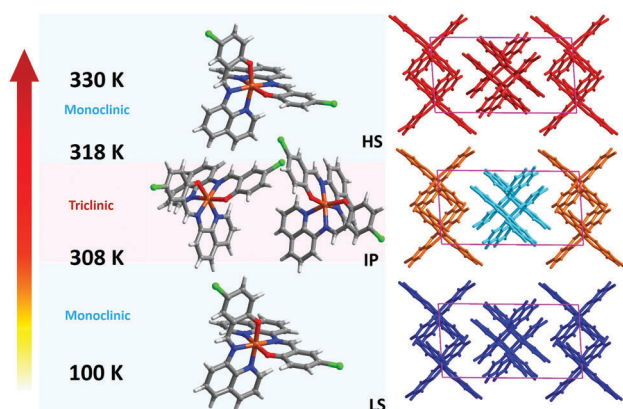
Fe–SCO compounds. The highest temperature noted previously was ∼250 K.

For a deeper comparison of a related symmetry breaking Fe(III) compound, $[Fe^{III}(qsal-Br)_2]NO_3 \cdot 2MeOH$,[35] **2** shows a two-step SCO with a large plateau of about 96 K while **1** has a small *pseudo*-plateau with width about 8 K. Consideration of intermediate state structures shows that compound **1** and **2** both have two Fe centres, 1LS–1HS. However, these Fe centres interact in different fashion. In the case of **1**, a plane of the same spin state of $[Fe(II)(qsal-Cl)_2]$ is formed *via* two sets of π–π and P4AE interactions. In contrast, a chain of the same Fe(III) molecules connect, solely, through two sets of π–π interactions (Fig S3, ESI†). As both of the compounds show re-entrant behaviour, chains of 1LS and 1HS Fe(III) moieties in the intermediate state have to propagate through the whole compound in 2D and 3D packing to revert to 1HS upon heating. Whereas the 2D-plane of Fe(II) molecules in **1** is more facile to induce two unique Fe(II) sheets reaching one Fe(II) centre with fully HS behaviour. Such differences possibly result in a significantly narrower intermediate phase temperature gap in **1**.

The effect of light irradiation on compound **1** was also studied. Irradiations at 405, 510, 650, 830 and 980 nm were tested with 650 nm irradiation inducing the most efficient photoconversion. The T(LIESST) curve was recorded. A common feature to **1** is the shape of the T(LIESST) curve. Increasing the temperature from 10 K in the dark, after photo-saturation was reached, induces an increase of the $\chi_M T$ value. This usually follows from the Fe(II) zero-field splitting.[42] After a maximum in the T(LIESST) curve, the $\chi_M T$ value drops down to the base line. Regarding the photoconversion efficiency, it is 30% with T(LIESST) = 40 K. An interesting point is that upon irradiation at 980 nm, a partial depopulation of the photo-induced HS state is observed, due to the reverse-LIESST process. Compared to the relaxation in the dark measured at 10 K (inset in Fig. 4), the reverse LIESST is clearly operative, even if it is not complete.

The ^{57}Fe Mössbauer spectra of **1** were measured at low (∼5 K) and room temperatures to confirm the presence of LS and HS forms. The spectral parameters of the compounds are shown in Fig. 5 and Table S5 (ESI†). The results are typical for Fe(II) complexes with quadrupole splitting, ΔE_Q, and isomer shift, δ of *ca.* 1 and 0.5 mm s^{-1} for LS forms while they are about 2 and 1 mm s^{-1} for HS forms, respectively.[43,44] For compound **1**, the fully Fe(II) LS forms exist at low temperatures. At room temperature, some fractions of Fe(II) HS are also present. These Mössbauer data correspond well with the magnetic results confirming exceptionally high $T_{1/2}$ in the compounds. Unfortunately, we cannot collect the fully HS Fe(II) spectrum as this occurs at too high a temperature for our Mössbauer facility.

Differential scanning calorimetry (DSC) data were collected on compound **1** using a 10 K min^{-1} scan rate. From the DSC plots in Fig. S4 (ESI†), there are two peaks for endo- and exothermic measurements. All the phase transition temperatures from the DSC data are in the same range as the spin transition results from magnetic measurements. As mentioned above, the initial magnetic plot for **1** roughly suggested a one-step SCO with an abrupt spin transition. The DSC result confirms the two step SCO present in this
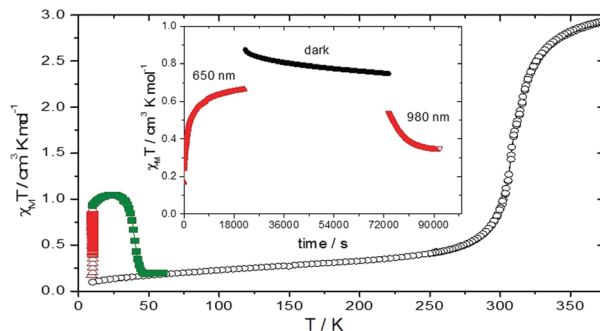

Fig. 4 Thermal behaviour of the $\chi_M T$ values for **1** in the dark (○), under a 650 nm irradiation (△) and after this irradiation in the dark at 0.4 K min^{-1} (■). The inset reports the time dependence of the $\chi_M T$ values in **1** following irradiation at 650 nm (▲) and 980 nm (▽) compared to the relaxation in the dark at 10 K (■).
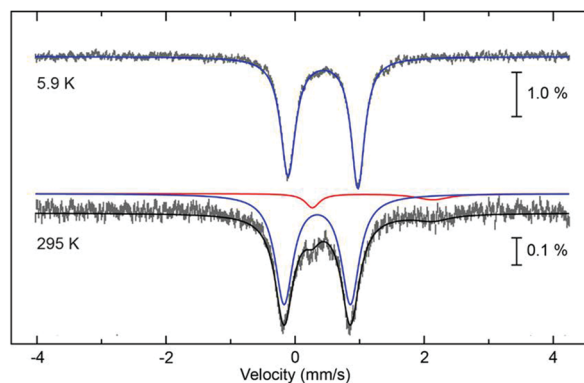

Fig. 5 Variable temperature ^{57}Fe Mössbauer spectral plots for **1**. At low temperature the sample is fully low spin (blue fit). At 295 K the sample is a mixture of low spin (blue) and high spin (red). Fitted parameters are given in Table S5 (ESI†).

compound. Moreover, the small ΔS value of 19.8 J mol^{-1} K^{-1} in **1**, agrees with data by Wang and Gao *et al.* who reported that symmetry breaking was also associated with a two-step SCO and led to a significant lowering in ΔH and ΔS values.[40]

In summary, $[Fe(II)(qsal-Cl)_2]$ **1** has provided an unprecedented array of magnetic and spin crossover properties. It is the first Fe(II) compound with a N_2O donor ligand to exhibit symmetry breaking accompanied by a two-step SCO above room temperature, the highest temperatures reported thus far for symmetry breaking SCO compounds (*viz.* $T_{1/2}$ = 308 and 316 K). In general, compared to iron(III) analogues $[Fe(III)(qsal-X)_2]Y$,[12,45] we propose that the abrupt SCO at such a high temperature in **1** is due to an absence of anions/solvents in the lattice that allow the Fe(II) molecules to have larger surface contact (*via* two extra sets of π–π and P4AE interactions) than for the Fe(III) complexes which enhances the strong cooperativity. Subsequently, to design a potential spin crossover material, the fundamental requirements for an abrupt spin crossover, particularly in Fe-qsal complexes, is the combination of the symmetrical two sets of π–π and P4AE interactions. To show spin transition at exceptionally high temperatures, the extra two sets of π–π and P4AE interactions are further recommended.

Notes and references

‡ Synthesis details and crystallographic data at variables temperatures are presented in the ESI.†

1 R. J. Deeth, C. M. Handley and B. J. Houghton, in *Spin-Crossover Materials*, ed. M. A. Halcrow, John Wiley & Sons Ltd, 2013, pp. 443–454.
2 P. N. Martinho, C. Rajnak and M. Ruben, in *Spin-Crossover Materials*, ed. M. A. Halcrow, John Wiley & Sons Ltd, 2013, pp. 375–404.
3 P. Gütlich, A. Hauser and H. Spiering, *Angew. Chem., Int. Ed. Engl.*, 1994, **33**, 2024–2054.
4 A. Bousseksou, G. Molnar, L. Salmon and W. Nicolazzi, *Chem. Soc. Rev.*, 2011, **40**, 3313–3335.
5 K. S. Murray, in *Spin-Crossover Materials*, ed. M. A. Halcrow, John Wiley & Sons Ltd, 2013, pp. 1–54.
6 M. A. Halcrow, *Chem. Commun.*, 2013, **49**, 10890–10892.
7 M. Nihei, T. Shiga, Y. Maeda and H. Oshio, *Coord. Chem. Rev.*, 2007, **251**, 2606.
8 P. Gütlich and H. A. Goodwin, in *Spin Crossover in Transition Metal Compounds I*, ed. P. Gütlich and H. A. Goodwin, Springer Berlin Heidelberg, Berlin, Heidelberg, 2004, pp. 1–47.
9 B. Weber, E. Kaps, J. Weigand, C. Carbonera, J.-F. Létard, K. Achterhold and F. G. Parak, *Inorg. Chem.*, 2008, **47**, 487–496.
10 B. Weber, W. Bauer and J. Obel, *Angew. Chem., Int. Ed.*, 2008, **47**, 10098–10101.
11 S. Dorbes, L. Valade, J. A. Real and C. Faulmann, *Chem. Commun.*, 2005, 69–71.
12 D. J. Harding, P. Harding and W. Phonsri, *Coord. Chem. Rev.*, 2016, **313**, 38–61.
13 B. Weber, *Coord. Chem. Rev.*, 2009, **253**, 2432–2449.
14 L. Zhang, G.-C. Xu, H.-B. Xu, V. Mereacre, Z.-M. Wang, A. K. Powell and S. Gao, *Dalton Trans.*, 2010, **39**, 4856–4868.
15 L. Zhang, G.-C. Xu, Z.-M. Wang and S. Gao, *Eur. J. Inorg. Chem.*, 2013, 1043–1048.
16 T. Romero-Morcillo, M. Seredyuk, M. C. Muñoz and J. A. Real, *Angew. Chem., Int. Ed.*, 2015, **54**, 14777–14781.
17 S. Hayami, Z.-z. Gu, H. Yoshiki, A. Fujishima and O. Sato, *J. Am. Chem. Soc.*, 2001, **123**, 11644–11650.
18 K. Takahashi, H. Mori, H. Kobayashi and O. Sato, *Polyhedron*, 2009, **28**, 1776–1781.
19 D. J. Harding, D. Sertphon, P. Harding, K. S. Murray, B. Moubaraki, J. D. Cashion and H. Adams, *Chem. – Eur. J.*, 2013, **19**, 1082–1090.
20 K. Fukuroi, K. Takahashi, T. Mochida, T. Sakurai, H. Ohta, T. Yamamoto, Y. Einaga and H. Mori, *Angew. Chem., Int. Ed.*, 2014, **53**, 1983–1986.
21 O. Iasco, E. Rivière, R. Guillot, M. Buron-Le Cointe, J.-F. Meunier, A. Bousseksou and M.-L. Boillot, *Inorg. Chem.*, 2015, **54**, 1791–1799.
22 K. Nakano, S. Kawata, K. Yoneda, A. Fuyuhiro, T. Yagi, S. Nasu, S. Morimoto and S. Kaizaki, *Chem. Commun.*, 2004, 2892–2893.
23 N. Bréfuel, H. Watanabe, L. Toupet, J. Come, N. Matsumoto, E. Collet, K. Tanaka and J.-P. Tuchagues, *Angew. Chem., Int. Ed.*, 2009, **48**, 9304–9307.
24 D. Chernyshov, M. Hostettler, K. W. Törnroos and H.-B. Bürgi, *Angew. Chem., Int. Ed.*, 2003, **42**, 3825–3830.
25 N. Ortega-Villar, M. Muñoz and J. Real, *Magnetochemistry*, 2016, **2**, 16.
26 D. Boinnard, A. Bousseksou, A. Dworkin, J. M. Savariault, F. Varret and J. P. Tuchagues, *Inorg. Chem.*, 1994, **33**, 271–281.
27 W. Bauer, T. Pfaffeneder, K. Achterhold and B. Weber, *Eur. J. Inorg. Chem.*, 2011, 3183–3192.
28 J. K. McCusker, A. L. Rheingold and D. N. Hendrickson, *Inorg. Chem.*, 1996, **35**, 2100–2112.
29 M. Marchivie, P. Guionneau, J.-F. Letard and D. Chasseau, *Acta Crystallogr., Sect. B: Struct. Sci.*, 2005, **61**, 25–28.
30 L. Zhang, G.-C. Xu, H.-B. Xu, T. Zhang, Z.-M. Wang, M. Yuan and S. Gao, *Chem. Commun.*, 2010, **46**, 2554–2556.
31 T. Kuroda-Sowa, Z. Yu, Y. Senzaki, K. Sugimoto, M. Maekawa, M. Munakata, S. Hayami and Y. Maeda, *Chem. Lett.*, 2008, **37**, 1216–1217.
32 T. M. Ross, B. Moubaraki, K. S. Wallwork, S. R. Batten and K. S. Murray, *Dalton Trans.*, 2011, **40**, 10147–10155.
33 H. Watanabe, N. Bréfuel, E. Collet, L. Toupet, K. Tanaka and J.-P. Tuchagues, *Eur. J. Inorg. Chem.*, 2013, 710–715.
34 S. Bonnet, M. A. Siegler, J. S. Costa, G. Molnar, A. Bousseksou, A. L. Spek, P. Gamez and J. Reedijk, *Chem. Commun.*, 2008, 5619–5621.
35 D. J. Harding, W. Phonsri, P. Harding, K. S. Murray, B. Moubaraki and G. N. L. Jameson, *Dalton Trans.*, 2015, **44**, 15079–15082.
36 D. J. Harding, W. Phonsri, P. Harding, I. A. Gass, K. S. Murray, B. Moubaraki, J. D. Cashion, L. Liu and S. G. Telfer, *Chem. Commun.*, 2013, **49**, 6340–6342.
37 K. Takahashi, T. Sato, H. Mori, H. Tajima and O. Sato, *Phys. B*, 2010, **405**, S65–S68.
38 D. Sertphon, D. J. Harding, P. Harding, K. S. Murray, B. Moubaraki, J. D. Cashion and H. Adams, *Eur. J. Inorg. Chem.*, 2013, 788–795.
39 V. Russell, M. Scudder and I. Dance, *J. Chem. Soc., Dalton Trans.*, 2001, 789–799.
40 W. Zhang, F. Zhao, T. Liu, M. Yuan, Z.-M. Wang and S. Gao, *Inorg. Chem.*, 2007, **46**, 2541–2555.
41 M. A. Halcrow, in *Spin-Crossover Materials*, ed. M. A. Halcrow, John Wiley & Sons Ltd, 2013, pp. 147–169.
42 J.-F. Letard, *J. Mater. Chem.*, 2006, **16**, 2550–2559.
43 P. Gütlich, Y. Garcia and H. A. Goodwin, *Chem. Soc. Rev.*, 2000, **29**, 419–427.
44 O. Hietsoi, P. W. Dunk, H. D. Stout, A. Arroyave, K. Kovnir, R. E. Irons, N. Kassenova, R. Erkasov, C. Achim and M. Shatruk, *Inorg. Chem.*, 2014, **53**, 13070–13077.
45 W. Phonsri, PhD thesis, Walailak University, Thailand, 2014.